

# Solvation Can Open the Photoisomerization Pathway for the Direct Photodissociation Reaction of Diiodomethane: Transient Resonance Raman Observation of the Isodiiodomethane Photoproduct from Ultraviolet Excitation of Diiodomethane in the Solution Phase

Xuming Zheng and David Lee Phillips\*

Department of Chemistry, The University of Hong Kong, Pokfulam Road, Hong Kong

Received: March 13, 2000; In Final Form: May 8, 2000

We report transient resonance Raman experiments that identify isodiiodomethane as the photoproduct responsible for the  $\sim 385$  nm absorption band observed following ultraviolet excitation of diiodomethane in liquid solutions. Comparison with previously reported gas-phase experiments and solution-phase resonance Raman and femtosecond transient absorption results suggest that solvation leads to appreciable production of the isodiiodomethane ( $\text{H}_2\text{C}-\text{I}-\text{I}$ ) photoproduct via the interaction of the initially formed  $\text{CH}_2\text{I}$  and  $\text{I}$  fragments with the solvent cage. The isodiiodomethane photoproduct is likely the species or an intermediate to the species that reacts with alkenes in cyclopropanation reactions that use ultraviolet excitation of diiodomethane in liquids.

## Introduction

The Simmons–Smith reaction for cyclopropanation uses diiodomethane as a reagent with a Zn–Cu couple.<sup>1</sup> In the solution phase, the photolysis of diiodomethane in the presence of olefins gives cyclopropanes with high stereospecificity.<sup>2</sup> The use of diiodomethane in cyclopropanation reactions has been refined and extended to a variety of molecules and solvent systems.<sup>3–5</sup> A number of intermediates such as an excited diiodomethane state, an iodonium–iodide ion pair or others have been proposed for the cyclopropanation reactions using diiodomethane as a reagent.<sup>1–5</sup>

Excitation of gas-phase diiodomethane with ultraviolet light ( $<5$  eV) leads to a direct photodissociation reaction that gives a  $\text{CH}_2\text{I}$  radical and an iodine atom in the ground state ( $\text{I}^2\text{P}_{3/2}$ ) or the spin–orbit excited state ( $\text{I}^*2\text{P}_{1/2}$ ).<sup>6–8</sup> Although it is energetically feasible to produce  $\text{CH}_2$  and  $\text{I}_2$  at wavelengths below 333 nm, this process is symmetry forbidden for the ultraviolet transitions<sup>9,10</sup> and only becomes appreciable at energies  $>6.4$  eV.<sup>11,12</sup> Flash photolysis experiments by Schmitt and Comes<sup>7</sup> have shown that ultraviolet excitation of diiodomethane in the gas phase leads predominantly to the  $\text{CH}_2\text{I} + \text{I}$  or  $\text{I}^*$  product channels and the  $\text{CH}_2 + \text{I}_2$  channel is at best a very minor one for ultraviolet excitation. Molecular beam experiments have shown that the ultraviolet photodissociation of diiodomethane in the gas phase occurs on a repulsive potential energy surface with a time much less than a rotational period.<sup>6,8</sup> Translational photofragment spectroscopy experiments indicate that the  $\text{CH}_2\text{I}$  photofragment receives substantial excitation of its internal degrees of freedom.<sup>8,13</sup> Vibrational energy distributions of the  $\text{CH}_2\text{I}$  photofragment were measured using infrared fluorescence experiments following ultraviolet excitation.<sup>14,15</sup> The quantum yield for production of  $\text{I}^*$  from the photodissociation of gaseous diiodomethane excited from 247.5 to 366.5 nm was also measured.<sup>9</sup>

In contrast to the relatively clear picture for the ultraviolet excitation of gas-phase diiodomethane that results in a direct photodissociation reaction of one C–I bond, the photochemistry

and dynamics are not very clear in condensed-phase environments such as solid matrices and liquid solutions despite a number of investigations. Excitation of condensed-phase diiodomethane with ultraviolet light<sup>16–19</sup> as well as direct photoionization<sup>20</sup> and radiolysis<sup>21,22</sup> all produce photoproducts that have characteristic absorption bands  $\sim 385$  nm (intense) and 570 nm (weak). A number of possible assignments have been put forward for the identity of these photoproducts: trapped electrons,<sup>16</sup> the cation of  $\text{CH}_2\text{I}_2$ ,<sup>20,22</sup> and the isomer of  $\text{CH}_2\text{I}_2$ .<sup>18,19</sup> One possible assignment suggested was the 385 nm absorption band is due to the  $\text{CH}_2\text{I}_2^+$  radical cation and the 570 nm band is due to the  $\text{CH}_2\text{I}$  radical.<sup>17,21</sup> The absorption spectrum of the  $\text{CH}_2\text{I}$  radical in the gas phase shows bands in the 200–400 nm region.<sup>23</sup> Maier and co-workers proposed an assignment of these absorption bands to isodiiodomethane ( $\text{H}_2\text{C}-\text{I}-\text{I}$ )<sup>18,19</sup> based on infrared absorption spectra obtained in low-temperature solid matrices following ultraviolet excitation of diiodomethane and the observation that the process appeared at least partly reversible when the photoproducts were further excited. The thermal stability of isodiiodomethane was also tested in low-temperature polyethylene matrices and started to disappear at temperatures above 100 K and the thermal stabilities of isobromoiodomethane and isochloroiodomethane were much lower.<sup>19</sup> Thus, it is not clear whether the isodihalomethane species will have any importance for reactions occurring in room-temperature liquid solutions.

Several research groups have investigated the short-time photodissociation dynamics of diiodomethane ultraviolet photodissociation in liquid solutions using femtosecond transient absorption spectroscopy.<sup>24–26</sup> These experiments monitored the photoproduct produced using 620,<sup>24</sup> 400,<sup>25</sup> and 290–1220 nm wavelengths.<sup>26</sup> Although, the transient absorption spectra from all three experiments displayed similar behavior (a fast rise followed by a fast decay and a slow rise), their results led to three different interpretations depending on the identity of the species attributed to the photoproducts. The interpretation of much of the photochemistry and ultrafast experimental work<sup>16–26</sup>

done for the ultraviolet excitation of diiodomethane in condensed phases is unclear because of the ambiguity about what photoproduct species is responsible for the  $\sim 385$  nm and  $\sim 570$  nm absorption bands observed in both solid matrices and liquid solutions. The identities of these photoproduct species are also important for better understanding the mechanism(s) of cyclopropanation reactions<sup>1–5</sup> involving solution-phase diiodomethane.

In this paper, we report transient resonance Raman experiments that unambiguously identify isodiiodomethane as the photoproduct that is mainly responsible for the  $\sim 385$  nm absorption formed following ultraviolet excitation of diiodomethane in liquid solutions. Density functional theory calculations of the optimized structures, vibrational frequencies and electronic absorption spectra are also reported for isodiiodomethane,  $\text{CH}_2\text{I}_2^+$ , and  $\text{CH}_2\text{I}$ . We compare our current solution-phase results with those previously found for the ultraviolet excitation of gas-phase diiodomethane and discuss the effects of solvation on the photochemistry of diiodomethane. We briefly discuss the implications for the mechanism of cyclopropanation reactions via ultraviolet excitation of diiodomethane in liquid solutions.

### Experiment and Calculations

Diiodomethane (99%), diiodomethane- $d_2$  (99%), and spectroscopic grade cyclohexane (99.9%) were purchased and used as received to prepare samples of about 0.20 M for the time-resolved resonance Raman experiments. The apparatus and methods for the time-resolved resonance Raman experiments have been given previously<sup>27–29</sup> and only a short description will be presented here. The hydrogen Raman shifted laser lines of the third harmonic (354.7 nm) of a nanosecond pulsed Nd:YAG laser provided the pump (309.1 nm) and probe (416.0 nm) excitation wavelengths for the time-resolved resonance Raman experiments. A near collinear geometry was used to focus the pump and probe laser beams onto a flowing liquid sample. Spectra were acquired with pump–probe time delays of 0, 10, and 20 ns using an optical delay between the pump and probe pulses. The transient resonance Raman spectra obtained for 0, 10, and 20 ns were very similar to one another. The Raman scattered light was collected with reflective optics using a backscattering geometry and imaged through a polarization scrambler and entrance slit of a 0.5 m spectrograph. The spectrograph grating dispersed the light onto a liquid nitrogen cooled CCD mounted on the exit port of the spectrograph. The Raman signal was collected by the CCD for 300–600 s before being read out to an interfaced PC computer. About 10 readouts were added together to obtain a resonance Raman spectrum. Pump only, probe only, and pump–probe transient Raman spectra as well as a background scan were acquired. Known Raman frequencies of the cyclohexane bands were used to calibrate the wavenumber shifts of the resonance Raman spectra. The solvent and parent diiodomethane bands were removed from the pump–probe transient spectrum by subtracting an appropriately scaled probe only resonance Raman spectrum. The pump only spectrum and background scan displayed no discernible bands in the probe spectral region.

All of the density functional calculations were performed using the Gaussian program suite.<sup>30</sup> Complete geometry optimization and vibrational frequency calculations were done analytically using a  $C_s$  symmetry constraint. The plane of symmetry contained the carbon and two iodine atoms. The double- $\zeta$  plus valence polarization for I and the triple- $\zeta$  plus valence polarization for carbon and hydrogen (DZVP-TZVP DFT basis)<sup>31,32</sup> and Sadlej triple- $\zeta$  plus valence polarization

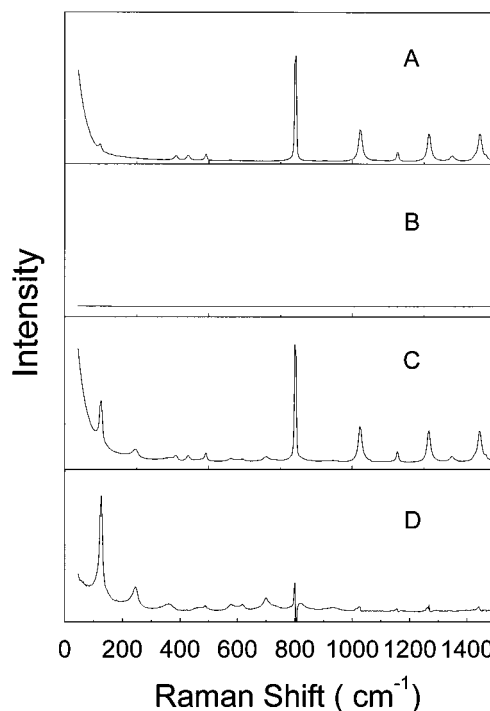


**Figure 1.** Examples of a typical 416.0 nm probe only Raman spectrum (A), 309.1 nm pump only spectrum in the probe wavelength region (B), a pump–probe Raman spectrum (C), and the resulting transient resonance Raman spectrum (D) of the diiodomethane photoproduct.

(Sadlej TZVP)<sup>32</sup> basis sets were used for the B3LYP density functional theory (DFT) calculations (structure and vibrational frequencies computations) and for the time-dependent density functional theory at random-phase approximation<sup>33</sup> calculations (TD(RPA)) to compute electronic transition energies. The DFT calculated vibrational frequencies likely have errors on the order of several percent (2–5%).<sup>31,32</sup>

### Results and Discussion

Our 309.1 nm pump excitation wavelength is very close to the 310 nm excitation used in two of the transient absorption experiments<sup>24,26</sup> and similar to ultraviolet excitation wavelengths (260–300 nm) used in several of the other experiments.<sup>17–19,25</sup> Thus, we expect to produce the diiodomethane photoproducts previously observed in the other photolysis experiments that have absorption bands  $\sim 385$  and  $\sim 570$  nm.<sup>16–22,24–26</sup> Åkesson and co-workers<sup>26</sup> previously noted that their 50–200 ps transient absorption spectrum of the diiodomethane photoproduct produced from 310 nm excitation of diiodomethane in acetonitrile solution was very similar to transient absorption spectra found for nanosecond ultraviolet photolysis of diiodomethane in acetonitrile,<sup>25</sup> in a 3-methylpentane matrix at 77 K,<sup>17</sup> and in argon/nitrogen matrices at 12 K.<sup>18,19</sup> Our probe wavelength of 416.0 nm was chosen to be resonant on the red side of the  $\sim 385$  nm transient absorption band<sup>16–22,24–26</sup> in order to acquire higher signal-to-noise transient resonance Raman spectra (probe wavelengths of 368.9 and 397.9 nm were also used and similar spectra were obtained for the photoproduct but with less signal-to-noise). Figure 1 shows a typical 416.0 nm probe only Raman spectrum, 309.1 nm pump only spectrum in the probe wavelength region, a pump–probe Raman spectrum, and the resulting transient resonance Raman spectrum of the diiodomethane photoproduct (obtained by subtracting the probe only spectrum from the pump–probe spectrum). All the data presented in Figure 1 are relative to the 416.0 nm probe laser. Figure 2 presents transient

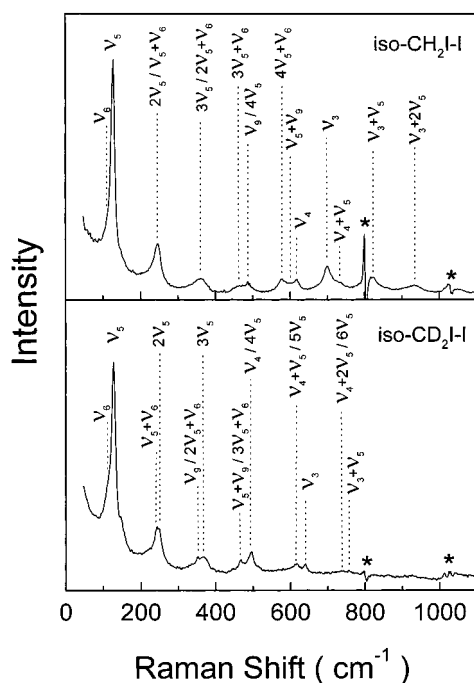


**Figure 2.** Transient resonance Raman spectra of the diiodomethane- $h_2$  ( $\text{CH}_2\text{I}_2$ ) and diiodomethane- $d_2$  ( $\text{CD}_2\text{I}_2$ ) photoproduct obtained using a 309.1 nm pump and 416.0 nm probe excitation wavelengths. The time delay between the pump and probe beams was  $\sim 10$  ns.

resonance Raman spectra of the diiodomethane photoproduct formed from 309.1 nm excitation of diiodomethane and diiodomethane- $d_2$  in cyclohexane solution. The transient resonance Raman spectra shown in Figure 2 have most of their intensity in the fundamentals, overtones, and combination bands of three or four Franck–Condon active modes whose fundamentals are at 701, 619, and 128  $\text{cm}^{-1}$  for diiodomethane- $h_2$  and 640, 496, 128, and  $\sim 110$   $\text{cm}^{-1}$  for diiodomethane- $d_2$ .

We have done density functional theory calculations to find the optimized geometries, vibrational frequencies, and electronic absorption transitions for the  $\text{CH}_2\text{I}$ , iso- $\text{CH}_2\text{I}_2$ , and  $\text{CH}_2\text{I}_2^+$  species. Table 1 lists the parameters for the optimized geometries of  $\text{CH}_2\text{I}$ , iso- $\text{CH}_2\text{I}_2$ , and  $\text{CH}_2\text{I}_2^+$  found for the B3LYP density functional theory calculations. Table 2 compares the experimental vibrational frequencies found from the transient resonance Raman spectra (this work) produced from ultraviolet excitation of diiodomethane in cyclohexane solution and infrared absorption spectra<sup>18,19</sup> obtained after ultraviolet excitation of diiodomethane in low-temperature solid matrices with the calculated B3LYP density functional theory results for iso- $\text{CH}_2\text{I}_2$ ,  $\text{CH}_2\text{I}_2^+$  and  $\text{CH}_2\text{I}$ . Inspection of Table 2 shows that the fundamental bands of the photoproduct observed in the resonance Raman spectra of Figure 2 have values that agree well with those predicted for the isodiiodomethane ( $\text{H}_2\text{C}-\text{I}-\text{I}$ ) molecule but not with either the  $\text{CH}_2\text{I}_2^+$  radical cation or  $\text{CH}_2\text{I}$  radical that have been proposed as photoproducts mainly responsible for the  $\sim 385$  nm photoproduct absorption band.<sup>16,17,20–22,24,25</sup> For example, the  $\text{CH}_2\text{I}$  radical has no low-frequency  $A_1$  vibrational mode in the 100–130  $\text{cm}^{-1}$  region that is obviously associated with the photoproduct observed in the resonance Raman spectra of Figure 2. Similarly, the  $\text{CH}_2\text{I}_2^+$  radical cation has only one  $A_1$  mode in the 500–800  $\text{cm}^{-1}$  region while the photoproduct has a 701  $\text{cm}^{-1}$  mode and a 619  $\text{cm}^{-1}$  mode that have combination bands with the 128  $\text{cm}^{-1}$  band. The observed vibrational bands assigned to the nominal C–I stretch ( $\nu_3$ ) and  $\text{CH}_2$  wag ( $\nu_4$ ) fundamentals of the photoproduct show excellent agreement with the infrared bands

**TABLE 1: Parameters for the Optimized Geometries Computed from the B3LYP Density Functional Theory Calculations for Iso- $\text{CH}_2\text{I}_2$ ,  $\text{CH}_2\text{I}$ , and  $\text{CH}_2\text{I}_2^+$  Species<sup>a</sup>**

parameter	B3LYP/TZVP	B3LYP/DZVP–I, TZVP–C,H
	Iso- $\text{CH}_2\text{I}_2$	
C–I <sub>1</sub>	1.957	1.979
I <sub>1</sub> –I <sub>2</sub>	3.042	3.073
C–H <sub>3</sub> and C–H <sub>4</sub>	1.091	1.083
C–I <sub>1</sub> –I <sub>2</sub>	118.2	119.1
I <sub>1</sub> –C–H <sub>3</sub> and I <sub>1</sub> –C–H <sub>4</sub>	119.1	118.9
H <sub>3</sub> –C–I <sub>1</sub> –I <sub>2</sub> and H <sub>4</sub> –C–I <sub>1</sub> –I <sub>2</sub>	90.0	90.0
$\text{CH}_2\text{I}_2^+$		
C–I <sub>1</sub> and C–I <sub>2</sub>	2.147	2.168
C–H <sub>3</sub> and C–H <sub>4</sub>	1.095	1.083
I <sub>1</sub> –C–I <sub>2</sub>	97.36	97.65
I <sub>1</sub> –C–H <sub>3</sub> , I <sub>1</sub> –C–H <sub>4</sub> , I <sub>2</sub> –C–H <sub>3</sub> , and I <sub>2</sub> –C–H <sub>4</sub>	110.6	110.5
H <sub>3</sub> –C–H <sub>4</sub>	115.2	116.0
H <sub>3</sub> –C–H <sub>4</sub> –I <sub>1</sub>	126.4	126.7
H <sub>3</sub> –C–H <sub>4</sub> –I <sub>2</sub>	–126.4	–126.7
I <sub>1</sub> –C–I <sub>2</sub> –H <sub>3</sub>	115.5	115.2
I <sub>1</sub> –C–I <sub>2</sub> –H <sub>4</sub>	–115.5	–115.2
$\text{CH}_2\text{I}$		
C–I	2.052	2.075
C–H <sub>1</sub> and C–H <sub>2</sub>	1.090	1.078
I–C–H <sub>1</sub> and I–C–H <sub>2</sub>	118.4	118.0
H <sub>1</sub> –C–H <sub>2</sub>	123.1	124.0
H <sub>1</sub> –C–H <sub>2</sub> –I	180.0	180.0

<sup>a</sup> Bond lengths are in Ångstroms, and bond angles are in degrees.

observed for isodiiodomethane in low-temperature solid matrices.<sup>18,19</sup> Furthermore, the isotopic shifts observed for the resonance Raman bands agree well with the isotopic shifts predicted from the density functional theory calculations and those reported for the infrared C–I stretch and  $\text{CH}_2$  wag bands (see Table 2).<sup>18,19</sup> These results strongly indicate that the  $\sim 385$  nm absorption band of the diiodomethane photoproduct is associated with an isodiiodomethane ( $\text{CH}_2\text{I}-\text{I}$ ) photoproduct species. Figure 3 presents a schematic diagram of the structure of the isodiiodomethane species.

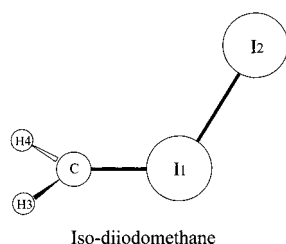
Table 3 shows the DFT computed charge distribution for the atoms (using Mulliken population analysis) in isodiiodomethane (iso- $\text{CH}_2\text{I}_2$ ), diiodomethane ( $\text{CH}_2\text{I}_2$ ), iodomethyl radical ( $\text{CH}_2\text{I}$ ), iodomethyl cation ( $\text{CH}_2\text{I}^+$ ), and the diiodomethane cation ( $\text{CH}_2\text{I}_2^+$ ). Comparison of the charge distributions for isodiiodomethane with the other species listed in Table 3 shows that isodiiodomethane has a charge distribution significantly different from that of diiodomethane or diiodomethane cation along the C–I bond. However, the isodiiodomethane charge distribution for the C–I bond is similar to that found for the iodomethyl cation, which suggests that the carbon atom and the  $\text{CH}_2\text{I}$  part of isodiiodomethane has some cation character and a reactivity similar to the iodomethyl cation. This may be part of the reason for the difficulty in assigning the species responsible for the  $\sim 385$  nm transient absorption band.

We have previously used B3LYP/3-21G\* time-dependent random-phase (TD/RPA) calculations to estimate the electronic transition energies for the ultraviolet absorption spectra of  $\text{CH}_2\text{I}_2$  and found reasonable agreement with the experimental spectra.<sup>34</sup> Similar calculations with larger basis sets are presented in Table 4 for the electronic absorption transitions of isodiiodomethane,  $\text{CH}_2\text{I}_2^+$  and  $\text{CH}_2\text{I}$ . Examination of Table 4 shows that neither the  $\text{CH}_2\text{I}_2^+$  radical cation or the  $\text{CH}_2\text{I}$  radical have computed electronic transitions in the 360–450 nm region where the  $\sim 385$  nm experimental absorption band of the photoproduct of diiodomethane appear. Both the  $\text{CH}_2\text{I}_2^+$  radical cation and  $\text{CH}_2\text{I}$

**TABLE 2: Comparison of the Experimental Vibrational Frequencies (in  $\text{cm}^{-1}$ ) Found from the Transient Resonance Raman Spectra (This Work) and Infrared Absorption Spectra (Refs 18 and 19) to the Calculated B3LYP Density Functional Theory Vibrational Frequencies<sup>a</sup>**

vibrational mode	B3LYP/Sadlej TZVP	B3LYP/DZVP-I, TZVP-C.H	resonance Raman (this work)	infrared absorption (refs 18 and 19)
		$\text{CH}_2\text{I}-\text{I}$ ( $\text{CD}_2\text{I}-\text{I}$ )		
$A'$ $\nu_1$ , $\text{CH}_2$ sym str	3131 (2260)	3174 (2289)		3028 (2213)
$\nu_2$ , $\text{CH}_2$ scissor	1340 (1011)	1384 (1037)		1373 (1041–1033)
$\nu_3$ , C–I str	755 (645)	733 (661)	701 (640)	714/705 (645)
$\nu_4$ , $\text{CH}_2$ wag	619 (476)	599 (460)	619 (496)	622–611 (498–486)
$\nu_5$ , I–I str	128 (128)	127 (126)	128 (128)	
$\nu_6$ , C–I–I bend	99 (93)	97 (92)	? (~110)	
$A''$ $\nu_7$ , $\text{CH}_2$ asym str	3281 (2451)	3326 (2486)		3151 (2378)
$\nu_8$ , $\text{CH}_2$ rock	865 (697)	888 (681)		
$\nu_9$ , $\text{CH}_2$ twist	447 (318)	441 (314)	487 ? (352 ?)	
		$\text{CH}_2\text{I}_2^+$		
$A_1$ $\nu_1$ , CH sym str	3103 (2246)	3162 (2271)		
$\nu_2$ , $\text{CH}_2$ def	1365 (1003)	1414 (1031)		
$\nu_3$ , CI sym str	551 (522)	537 (511)		
$\nu_4$ , ICI bend	114 (114)	113 (113)		
$B_1$ $\nu_5$ , CH asym str	3220 (2401)	3286 (2431)		
$\nu_6$ , $\text{CH}_2$ rock	755 (576)	784 (597)		
$A_2$ $\nu_7$ , $\text{CH}_2$ twist	983 (696)	1003 (709)		
$B_2$ $\nu_8$ , $\text{CH}_2$ wag	1080 (813)	1120 (838)		
$\nu_9$ , CI asym str	517 (490)	503 (480)		
		$\text{CH}_2\text{I}$		
$A_1$ $\nu_1$ , CH sym str	3126 (2252)	3174 (2285)		
$\nu_2$ , $\text{CH}_2$ def	1309 (974)	1353 (1006)		
$\nu_3$ , C–I str	614 (576)	609 (573)		
$B_1$ $\nu_4$ , $\text{CH}_2$ wag	234 (180)	166 (129)		
$B_2$ $\nu_5$ , CH asym str	3288 (2457)	3335 (2494)		
$\nu_6$ , $\text{CH}_2$ rock	832 (619)	855 (635)		

<sup>a</sup> The corresponding vibrational frequencies for deuterated isodiiodomethane are given in parentheses. str = stretch; sym = symmetric; asym = asymmetric; def = deformation;

**Figure 3.** Schematic diagram of the optimized geometry of isodiiodomethane with the atoms numbered as in Tables 1 and 3.

radical have moderate strength absorption bands computed at 341 and 316 nm, respectively. One (or two) intense electronic absorption transitions are calculated for the isodiiodomethane ( $\text{CH}_2\text{I}-\text{I}$ ) species in the 400 nm region, and this correlates reasonably well to the  $\sim 385$  nm intense absorption band from the photoproduct formed following ultraviolet light excitation of diiodomethane in condensed-phase environments.<sup>16–22,24–26</sup> Our present transient resonance Raman observation of the photoproduct demonstrates clearly that the isodiiodomethane species is mostly responsible for the  $\sim 385$  nm transient absorption band observed after ultraviolet excitation of diiodomethane in liquid solutions (at least on the ns time scale), and this is consistent with the DFT calculated electronic transition energies for isodiiodomethane.

Several experimental results suggest that the same species may be responsible for both the intense 385 nm and weaker 570 nm transient absorption bands. It is interesting to note that the kinetics associated with the ultrafast transient absorption experiments done with a 620 nm probe wavelength<sup>24</sup> and a 310 nm probe wavelength<sup>25</sup> are very similar to one another, which suggests they may be observing different transitions of the same photoproduct. Similarly, the most recent ultrafast transient absorption experiments<sup>26</sup> show that both the  $\sim 400$  and  $\sim 570$

nm absorption transients have similar dynamics and were attributed to the same photoproduct species and it was suggested that this species was probably isodiiodomethane. In low-temperature matrices, excitation within either the 370 nm intense absorption band ( $\sim 385$  nm in liquids) or the 545 nm ( $\sim 570$  nm in liquids) weak absorption bands leads to disappearance of these absorption bands and an almost quantitative reformation for the parent diiodomethane molecule.<sup>18,19</sup> This behavior and the very similar kinetics of both of the transient absorption bands suggests that the isodiiodomethane photoproduct may be responsible for both of the  $\sim 385$  and  $\sim 570$  nm transient absorption bands observed in the solution phase. We have done some additional DFT calculations to see if the weaker  $\sim 570$  nm absorption band can be assigned to an electronic transition of isodiiodomethane. Table 4 shows that some triplet-state electronic transitions in the 550–600 nm region for isodiiodomethane appear to correlate well with the experimental  $\sim 570$  nm weak absorption band. With our present level of theory, we were not able to calculate the similar electronic transitions for the  $\text{CH}_2\text{I}$  radical and  $\text{CH}_2\text{I}_2^+$  cation readily and these species could also have triplet-state transitions in the 550–600 nm region. We also note that errors for the DFT TD (RPA) electronic transitions energies can be somewhat large, and this makes it difficult to make accurate assignments. For example, Bauernschmitt and Alrichs<sup>33</sup> found the B3LYP/TD(RPA) calculations gave results consistently 0.5 eV below the experimental values for systems they examined while we found errors of about 0.15 to 0.3 eV for the ultraviolet transitions of  $\text{CH}_2\text{I}_2$ .<sup>34</sup> If the errors are fairly large for isodiiodomethane, then an alternative assignment could be the calculated  $\text{CH}_2\text{I}_2^+$  752 nm absorption to the experimental 570 nm absorption band and the isodiiodomethane 517 nm triplet transition to the  $\sim 385$  nm experimental absorption band. However, we do not consider

**TABLE 3: Charge Distributions for Isodiodomethane (iso-CH<sub>2</sub>I<sub>2</sub>), Diiodomethane (CH<sub>2</sub>I<sub>2</sub>), Iodomethyl Radical (CH<sub>2</sub>I), Iodomethyl Cation (CH<sub>2</sub>I<sup>+</sup>), and the Diiodomethane Cation (CH<sub>2</sub>I<sub>2</sub><sup>+</sup>) Computed from Density Functional Theory (B3LYP/Sadlej TZVP) Calculations<sup>a</sup>**

isodiodomethane (iso-CH <sub>2</sub> I <sub>2</sub> )		diiodomethane (CH <sub>2</sub> I <sub>2</sub> )		iodomethyl radical (CH <sub>2</sub> I)		diiodomethane cation (CH <sub>2</sub> I <sub>2</sub> <sup>+</sup> )		iodomethyl cation (CH <sub>2</sub> I <sup>+</sup> )	
atom	total atomic charge	atom	total atomic charge	atom	total atomic charge	atom	total atomic charge	atom	total atomic charge
C	0.82	C	-0.80	C	0.73	C	0.12	C	0.76
I <sub>1</sub>	0.82	I	0.30	I	0.47	I	0.83	I	1.05
I <sub>2</sub>	-0.26	I	0.30	H	-0.60	I	0.83	H	-0.40
H <sub>3</sub>	-0.69	H	0.10	H	-0.60	H	-0.39	H	-0.40
H <sub>4</sub>	-0.69	H	0.10			H	-0.39		

<sup>a</sup> The computed total atomic charges are listed for each atom.

**TABLE 4: Electronic Absorption Transition Energies Obtained from Density Functional Theory Calculations for Iso-CH<sub>2</sub>I<sub>2</sub>, CH<sub>2</sub>I<sub>2</sub><sup>+</sup>, and CH<sub>2</sub>I<sup>a</sup>**

molecule	electronic absorption transition energies (nm)	
	URPA//UB3LYP/Sadlej TZVP	URPA//UB3LYP/DZVP-I, TZVP-C,H
iso-CH <sub>2</sub> I <sub>2</sub>	triplet transitions	
	551 (0.0)	573 (0.0)
	517 (0.0)	544 (0.0)
	364 (0.0)	368 (0.0)
	336 (0.0)	341 (0.0)
	316 (0.0)	321 (0.0)
	singlet transitions	
	443 (0.0002)	463 (0.0003)
	425 (0.4023)	437 (0.2690)
	404 (0.0772)	423 (0.2657)
	284 (0.0002)	290 (0.0001)
280 (0.0230)	271 (0.0659)	
208 (0.0671)	191 (0.0044)	
CH <sub>2</sub> I <sub>2</sub> <sup>+</sup>	2648 (0.1250)	3856 (0.1321)
	1004 (0.0003)	1060 (0.0003)
	753 (0.0000)	777 (0.0000)
CH <sub>2</sub> I	341 (0.0003)	344 (0.0005)
	316 (0.0001)	311 (0.0002)
	262 (0.0001)	254 (0.0000)
	216 (0.0009)	210 (0.0001)

<sup>a</sup> Calculated transition oscillator strengths are in parentheses.

this alternative assignment to be likely for the following reasons. First, the experimental ~385 nm absorption band is very strong and unlikely to be associated with a triplet transition that would be expected to be weak. Second, two different species would be unlikely to give almost identical disappearance of both bands to re-form the parent diiodomethane molecule following excitation of either absorption band.<sup>18,19</sup> Further work using direct experimental probes of the 570 nm transition and/or more sophisticated theory and computations are needed unambiguously to assign the species responsible for the 570 nm transient absorption observed following ultraviolet excitation of diiodomethane in the solution phase.

Since we have clearly identified isodiodomethane as the photoproduct species primarily responsible for the ~385 nm transient absorption (at least on the ns time scale), we can now obtain a clearer general picture of the solution-phase dynamics and associated photochemistry following ultraviolet excitation of diiodomethane. The initial reaction coordinate following ultraviolet excitation (in the 330–360 nm region) of diiodomethane has been characterized with resonance Raman investigations in both the gas<sup>35–39</sup> and solution phases.<sup>36,37</sup> Excitation within the first absorption band for gas-phase diiodomethane results in both C–I bonds lengthening to the same degree accompanied by the I–C–I angle decreasing, a larger H–C–I angle, and a smaller H–C–H angle in the Franck–Condon region.<sup>37</sup> In the gas phase, the two C–I bonds appear equivalent to one another in the Franck–Condon region, which indicates that the molecule determines which C–I bond

is broken after the wave packet leaves the Franck–Condon region of the excited-state surface. The solution-phase resonance Raman spectra display significant intensity in the I–C–I antisymmetric stretch fundamental, odd overtones, and/or combination bands of the fundamental with other modes that are not present in the corresponding gas-phase resonance Raman spectra.<sup>35–37</sup> Resonance Raman intensity analysis of the solution-phase spectra reveals that the two C–I bonds lengthen by substantially different amounts (e.g., one much faster than the other) accompanied by a decrease in the I–C–I and H–C–H angles and a larger I–C–H angle. The two C–I bonds are not equivalent in the solution phase, and the solvent environment at the time of photoexcitation appears to choose which of the two C–I bonds will be cleaved (and likely collide with the solvent cage first). This solvent-induced symmetry breaking during the initial stages following photoexcitation is likely important to solvation opening up the photoisomerization pathway for the ultraviolet excitation of diiodomethane in the solution phase. For example, if the initial dynamics were similar to that found for the gas phase, then both C–I bonds would likely collide with the solvent cage at almost the same time with similar energetics. This would probably give similar recombination dynamics for both C–I bonds and would not be likely to form significant amounts of isodiodomethane. On the other hand, the solvent-induced symmetry breaking would primarily lead to one iodine atom colliding with the solvent cage first and recombination of the CH<sub>2</sub>I and I fragments within the solvent cage would lead to isodiodomethane (CH<sub>2</sub>I–I) or the parent molecule. The latest femtosecond experiments by Åkesson and co-workers<sup>26</sup> provide support for this hypothesis and are consistent with the Franck–Condon region dynamics we previously found from resonance Raman experiments.<sup>36,37</sup> The sharper 350 nm subband (probably due to CH<sub>2</sub>I photoproduct) appearance at ~0.5 ps in their transient absorption spectra is somewhat earlier than the ~1 ps appearance of the isodiodomethane photoproduct absorption ~385 nm.<sup>26</sup> This suggests that the isodiodomethane photoisomerization results from recombination of CH<sub>2</sub>I and I within the solvent cage. Thus, solvation is probably responsible for the photoisomerization process and this is consistent with the lack of a corresponding photoisomerization in the gas phase where only the direct photodissociation of diiodomethane into CH<sub>2</sub>I and iodine fragments is observed following ultraviolet excitation of diiodomethane.<sup>6–10,13–15</sup> After interaction with the solvent cage it appears that the isodiodomethane photoproduct undergoes vibrational relaxation of a 10 ps time scale.<sup>26</sup> Much work remains to be done in order to better understand the details of the formation of the isodiodomethane and CH<sub>2</sub>I photoproducts formed from ultraviolet excitation of diiodomethane in liquid solutions. We note that our present work only clearly identifies the isodiodomethane photoproduct on the nanosecond time scale and suggests that the mechanism of Åkesson<sup>26</sup> is correct insofar as the transient absorption ~385 nm on the ultrafast time scales

is the same as that observed on the nanosecond time scale. The  $\sim 385$  nm transient absorption band seen in the nanosecond time scale is very similar to that seen in the ultrafast experiments,<sup>25,26</sup> and it seems likely that they are due to the same species. However, we cannot distinguish between formation of the nanosecond isodiiodomethane photoproduct from recombination of a  $\text{CH}_2\text{I}$  radical and an I atom and formation via recombination of a  $\text{CH}_2\text{I}^+$  carbocation and an  $\text{I}^-$  anion. It would be very useful for ultrafast resonance Raman or infrared absorption experiments to be done to establish clearly the exact mechanism(s) of formation of the longer lived isodiiodomethane photoproduct. On the basis of the available experimental data at this time, we think that the  $\text{CH}_2\text{I}$  radical plus I atom recombination mechanism is more probable in nonpolar (and possibly polar) solvents.

There are noticeable solvent effects on resonance Raman spectra of diiodomethane in different solvents,<sup>37</sup> and it is not clear how the solvent environment influences the photodissociation/photoisomerization reactions of diiodomethane. In addition, the details of the short-time dynamics of these reactions remain to be elucidated. A combination of further theoretical as well as experimental work (both time-resolved techniques and frequency domain experiments) should prove useful in better understanding the finer points of the solution-phase dynamics at times less than several picoseconds. The solution-phase diiodomethane photophysics/photochemistry after ultraviolet photoexcitation can likely provide a valuable model to study solvent-solute interactions and caging effects on chemical reactions.

Since the photoproduct is formed within several picoseconds<sup>24-26</sup> and forms a relatively long-lived isodiiodomethane photoproduct on the order of nanoseconds or longer (ref 25 and this work), we expect that the isodiiodomethane species reacts with (or is an intermediate of the species that reacts with) alkenes in the cyclopropanation reactions using ultraviolet excitation of diiodomethane. The high level of selectivity and absence of C-H insertion for the cyclopropanation reactions using ultraviolet excitation of diiodomethane suggests that the reaction intermediate is not a free carbene.<sup>2-5</sup> This is consistent with the hypothesis that isodiiodomethane is the species that reacts with alkenes in the cyclopropanation reactions induced by ultraviolet excitation of diiodomethane, and it is conceivable that isodiiodomethane has a similar reactivity toward alkenes as the iodomethyl cation (whose charge distribution the isodiiodomethane  $\text{CH}_2\text{I}$  group closely resembles; see Table 3) or the methylene radical. Further work is in progress to investigate the probable reaction of isodiiodomethane or other longer lived photoproduct species with alkenes to produce cyclopropanated products.

There have also been interesting observations of new intermediates formed following ultraviolet excitation of diiodomethane in the presence of alkenes or in the presence of a small amount of polar solvent like ethanol in 77 K hydrocarbon glasses.<sup>16,40,41</sup> These intermediates were assigned to molecular halogen-alkene complexes (such as  $\text{I}_2$ -alkene)<sup>16</sup> for the experiments done in the presence of different alkenes and to trihalide ions (such as  $\text{I}_3^-$ ) when a trace amount of ethanol was also present.<sup>40</sup> We are currently investigating these intriguing reactions with transient resonance Raman experiments, and results will be reported in due course.

**Acknowledgment.** This work was supported by grants from the Committee on Research and Conference Grants (CRCG), the Research Grants Council (RGC) of Hong Kong, the Hung

Hing Ying Physical Sciences Research Fund and the Large Items of Equipment Allocation 1993-94 from the University of Hong Kong.

## References and Notes

- (1) Simmons, H. E.; Smith, R. D. *J. Am. Chem. Soc.* **1959**, *81*, 4256-4264.
- (2) Blomstrom, D. C.; Herbig, K.; Simmons, H. E. *J. Org. Chem.* **1965**, *30*, 959-964.
- (3) Pienta, N. J.; Kropp, P. J. *J. Am. Chem. Soc.* **1978**, *100*, 655-657.
- (4) Kropp, P. J.; Pienta, N. J.; Sawyer, J. A.; Polniaszek, R. P. *Tetrahedron* **1981**, *37*, 3229-3236.
- (5) Kropp, P. J. *Acc. Chem. Res.* **1984**, *17*, 131-137.
- (6) Kawasaki, M.; Lee, S. J.; Bersohn, R. *J. Chem. Phys.* **1975**, *63*, 809-814.
- (7) Schmitt, G.; Comes, F. J. *J. Photochem.* **1980**, *14*, 107-123.
- (8) Kroger, P. M.; Demou, P. C.; Riley, S. J. *J. Chem. Phys.* **1976**, *65*, 1823-1834.
- (9) Koffend, J. B.; Leone, S. R. *Chem. Phys. Lett.* **1981**, *81*, 136-141.
- (10) Cain, S. R.; Hoffman, R.; Grant, R. *J. Phys. Chem.* **1981**, *85*, 4046-4051.
- (11) Marvet, U.; Dantus, M. *Chem. Phys. Lett.* **1996**, *256*, 57-62.
- (12) Zhang, Q.; Marvet, U.; Dantus, M. *J. Chem. Phys.* **1998**, *109*, 4428-4442.
- (13) Jung, K.-W.; Ahmadi, T. S.; El-Sayed, M. A. *Bull. Korean Chem. Soc.* **1997**, *18*, 1274-1280.
- (14) Baughcum, S. L.; Hafmann, H.; Leone, S. R.; Nesbitt, D. J. *Faraday Discuss. Chem. Soc.* **1979**, *67*, 306-315.
- (15) Baughcum, S. L.; Leone, S. R. *J. Chem. Phys.* **1980**, *72*, 6531-6545.
- (16) Simons, J. P.; Tatham, P. E. R. *J. Chem. Soc. A* **1966**, 854-859.
- (17) Mohan, H.; Rao, K. N.; Iyer, R. M. *Radiat. Phys. Chem.* **1984**, *23*, 505-508.
- (18) Maier, G.; Reisenauer, H. P. *Angew. Chem., Int. Ed. Engl.* **1986**, *25*, 819-822.
- (19) Maier, G.; Reisenauer, H. P.; Hu, J.; Schaad, L. J.; Hess, B. A., Jr. *J. Am. Chem. Soc.* **1990**, *112*, 5117-5122.
- (20) Andrews, L.; Prochaska, F. T.; Ault, B. S. *J. Am. Chem. Soc.* **1979**, *101*, 9-15.
- (21) Mohan, H.; Iyer, R. M. *Radiat. Eff.* **1978**, *39*, 97-101.
- (22) Mohan, H.; Moorthy, P. N. *J. Chem. Soc., Perkin Trans. 2* **1990**, 277-282.
- (23) Sehested, J.; Ellermann, T.; Nielsen, O. J. *Int. J. Chem. Kinet.* **1994**, *26*, 259-272.
- (24) Schwartz, B. J.; King, J. C.; Zhang, J. Z.; Harris, C. B. *Chem. Phys. Lett.* **1993**, *203*, 503-508.
- (25) Saitoh, K.; Naitoh, Y.; Tominaga, K.; Yoshihara, K. *Chem. Phys. Lett.* **1996**, *262*, 621-626.
- (26) Tarnovsky, A. N.; Alvarez, J.-L.; Yartsev, A. P.; Sundström, V.; Åkesson, E. *Chem. Phys. Lett.* **1999**, *312*, 121-130.
- (27) Shoute, L. C. T.; Pan, D.; Phillips, D. L. *Chem. Phys. Lett.* **1998**, *290*, 24-28.
- (28) Pan, D.; Phillips, D. L. *J. Phys. Chem. A* **1999**, *103*, 4737-4743.
- (29) Pan, D.; Shoute, L. C. T.; Phillips, D. L. *J. Phys. Chem. A* **1999**, *103*, 6851-6861.
- (30) (a) Frisch, M. J.; Trucks, G. W.; Schlegel, H. B.; Scuseria, G. E.; Robb, M. A.; Cheeseman, J. R.; Zakrzewski, V. G.; Montgomery, J. A.; Stratmann, R. E.; Burant, J. C.; Dapprich, S.; Millam, J. M.; Daniels, A. D.; Kudin, K. N.; Strain, M. C.; Farkas, O.; Tomasi, J.; Barone, V.; Cossi, M.; Cammi, R.; Mennucci, B.; Pomelli, C.; Adamo, C.; Clifford, S.; Ochterski, J.; Perterson, G. A.; Ayala, P. Y.; Cui, Q.; Morokuma, K.; Mailick, D. K.; Rabuck, A. D.; Raghavachari, K.; Foresman, J. B.; Cioslowski, J.; Orvitz, J. V.; Stefanov, B. B.; Liu, G.; Liashenko, A.; Piskorz, P.; Komaromi, I.; Gomperts, R.; Martin, R. L.; Fox, D. J.; Kieth, T.; Al-laham, M.-A.; Peng, C. Y.; Nanayakkara, A.; Gonzalez, C.; Challacombe, M.; Gill, P. M. W.; Johnson, B. G.; Chen, W.; Wong, M. W.; Andres, J. L.; Head-Gordon, M.; Perlogle, E. S.; Pople, J. A. *Gaussian 98*, Revision A.1; Gaussian, Inc.: Pittsburgh, PA, 1998. (b) Becke, A. D. *J. Chem. Phys.* **1993**, *98*, 1372-1377.
- (31) Godbout, N.; Salahub, D. R.; Andzelm, J.; Wimmer, E. *Can. J. Chem.* **1992**, *70*, 560. Basis sets were obtained from the Extensible Computational Chemistry Environment Basis Set Database, Environmental and Molecular Sciences Laboratory which is part of the Pacific Northwest Laboratory, P.O. Box 999, Richland, WA 99352, and funded by the U.S. Department of Energy. The Pacific Northwest Laboratory is a multiprogram laboratory operated by Battelle Memorial Institute for the U.S. Department of Energy under contract DE-AC06-76RLO 1830. Contact David Feller or

Karen Schuchardt (Pacific Northwest Laboratory) for further information.

- (32) Sadlej, A. J. *Theor. Chim. Acta* **1992**, *81*, 339–354.
- (33) Bauernschmitt, R.; Ahlrichs, R. *Chem. Phys. Lett.* **1996**, *256*, 454–464.
- (34) Zheng, X.; Phillips, D. L. *Chem. Phys. Lett.* **2000**, *316*, 524–530.
- (35) Zhang, J.; Imre, D. G. *J. Chem. Phys.* **1988**, *89*, 309–313.
- (36) Kwok, W. M.; Phillips, D. L. *Chem. Phys. Lett.* **1995**, *235*, 260–267.

- (37) Kwok, W. M.; Phillips, D. L. *J. Chem. Phys.* **1996**, *104*, 2529–2540.
- (38) Duschek, F.; Schmitt, M.; Vogt, P.; Materny, A.; Kiefer, W. *J. Raman Spectrosc.* **1997**, *28*, 445–453.
- (39) Braun, M.; Materny, A.; Schmitt, M.; Kiefer, W.; Engel, V. *Chem. Phys. Lett.* **1998**, *284*, 39–46.
- (40) Brown, G. P.; Simons, J. P. *Trans. Faraday Soc.* **1969**, *65*, 3245.
- (41) Comments by Simons, J. P. in *Faraday Discuss.* **1997**, *108*, 93.